Available online at www.sciencedirect.com
SCIENCE DIRECT®
Journal of Hydrology 285 (2004) 114–124
Journal of Hydrology
www.elsevier.com/locate/jhydrol

Modelling streaming potential (SP) signals induced by water movement in the vadose zone

Mathieu Darnet*, Guy Marquis

Ecole et Observatoire des Sciences de la Terre, Institut de Physique du Globe de Strasbourg, 5 rue René Descartes, UMR 7516, Strasbourg F-67084, France

Received 20 November 2002; accepted 1 August 2003

Abstract

Field estimation of soil water flux has a direct application for water resource management. Standard methods are often difficult to apply because of the heterogeneity of the subsurface. In the present study, we show that Streaming Potential (SP) monitoring can provide a cost-effective tool to help estimate the nature of the hydraulic transfers (infiltration or evaporation) in the vadose zone. We have modelled the SP response of rainfall infiltration and evaporation in an unsaturated porous medium; our model shows that SP signals of several millivolts are generated, i.e. easily recordable with standard SP equipment and that they allow to characterize the upward or downward water flux. We have compared our model results to SP and hydraulic data sets acquired during both rainfall infiltration and evaporation phases and they confirmed that SP measurements allow effectively to estimate the direction of the water flux at the scale of the electrode separation (usually several decimetres), i.e. at a much larger scale than tensiometric measurements.

Keywords: Streaming potential; Water movement; Vadose zone; Electrical method

1. Introduction

Reliable medium-scale (several meters) field estimates of soil water fluxes using standard hydrological methods (e.g. tensiometry) are often difficult to obtain because of the heterogeneous nature of the subsurface. These methods provide only local estimates of hydraulic parameters and the installation of the sensors itself may increase the degree of heterogeneity. Geophysical methods provide minimally invasive tools that give helpful information to help estimate water fluxes in the vadose zone. The most commonly used geophysical techniques for water detection in saturated or unsaturated media are electrical soundings (Hagrey and Michaelsen, 1999; French et al., 2002; Kemna et al., 2002), ground-penetrating radar (Hagrey et al., 1999; Schmalz et al., 2002; Stoffregen et al., 2002), nuclear magnetic resonance imaging (Legchenko et al., 2002; Herrmann et al., 2002) and Streaming Potential (SP) measurements (Titov et al., 2002).

All these methods detect the presence of water in soils by detecting changes in ground physical properties (e.g. electrical conductivity, dielectric

* Corresponding author. Fax: +33-390-2401-25.
E-mail addresses: mathieu.darnet@eost.u-strasbg.fr (M. Darnet); guy.marquis@eost.u-strasbg.fr (G. Marquis).

0022-1694/$ - see front matter © 2003 Elsevier B.V. All rights reserved.
doi:10.1016/j.jhydrol.2003.08.010

permittivity) but only the SP method is sensitive to actual water flow. Indeed, the SP method consists in measuring natural electric potential variations generated by the electrokinetic effect of the underground fluid flow. Thus, the spatial distribution of electric potential may allow to map the steady-state flow (Ogilvy et al., 1969; Bogoslovsky and Ogilvy, 1970, 1973). This flow map in fact describes the geometry of the singularities in the flow but does not provide information about its dynamics that can only be studied through time monitoring of SP variations.

SP monitoring consists of the continuous measurement of electric potential differences between two unpolarizable electrodes (Petiau, 2000) with a high-impedance voltmeter (Fig. 1). This dipole is usually along the direction of the water flow. In addition, to ensure a good electrical contact between the electrode and the medium, an electrically conductive solution (e.g. salty water with clay) is usually added around the electrode.

Can we use this cost-effective technique for monitoring water flow in unsaturated media? Thony et al. (1997) obtained through an experiment a linear relationship between SP values and unsaturated soil water flux. Doussan et al. (2002) tested experimentally the existence and robustness of such a flux–SP relationship for different soil types and pedoclimatic conditions: they observed that time variations of SP were correlated to both rainfall events and evaporation but that the linear relationship between SP and unsaturated water fluxes is not always valid.

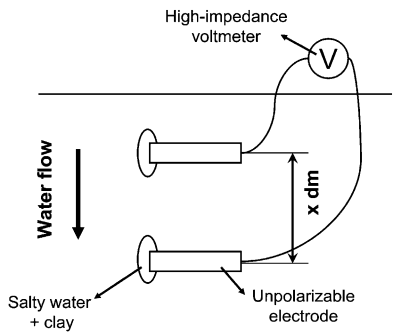

Fig. 1. Sketch of a standard streaming potential experiment for the monitoring of vertical water flow. A high-impedance voltmeter is used to measure the electric potential differences between two unpolarizable electrodes. This dipole is usually along the direction of the water flow. In addition, to ensure a good electrical contact between the electrode and the medium, an electrically conductive solution (e.g. salty water with clay) is usually added around the electrode.

The aim of our study is to develop a model, based on the electrokinetic effect of rainfall infiltration and evaporation, that explains physically the relationship between SP variations and unsaturated soil water flux. To investigate this matter, we modelled the SP signals produced by rain water infiltration in the vadose zone. We then compared our model results to the data of Thony et al. (1997) and Doussan et al. (2002) to determine which features can be identified from SP measurements.

2. Modeling of streaming potential variations induced by rainfall infiltration and evaporation

SP are electric potentials generated by electrokinetic processes when an electrolyte flows in a porous medium. We present here briefly the electrokinetic theory relevant to geophysical applications: the reader is referred to Revil and Pezard (1999a) and Revil et al. (1999b) and the references therein for more details. A pore fluid is in chemical equilibrium with the rock matrix, resulting in an ion accumulation at the rock/fluid interface known as the electrical double layer (EDL). Thus, when a fluid flows through a porous medium, so do the charged ionic species, resulting in the generation of a drag current. If no other external electric current sources exist, this so-called convection current is balanced by a conduction current so as to maintain a constant electric charge. The conduction current is responsible for the SP. In this case, the electric potential V is related to the fluid pressure P through the Helmholtz–Smoluchowski equation

$$\bar{\nabla}V = C\bar{\nabla}P \tag{1}$$

where C the SP cross-coupling coefficient (V Pa^{-1}). For unsaturated water flow in a silica-dominated porous material with negligible surface electrical conductivity, C is (Revil et al., 1999b)

$$C = \frac{\varepsilon_f \zeta}{\eta_f \sigma_f S_w^n} \tag{2}$$

where S_w is the effective water content, σ_f, ε_f and η_f, are respectively, the electrical conductivity (S m^{-1}), dielectric permittivity (F m^{-1}) and dynamic viscosity

(Pa s) of the fluid, ζ is the zeta potential (V) and n is the second Archie exponent (usually close to 2, Revil et al., 1999b). For soils of high clay content (e.g. loamy soil), we should add a second-order term to Eq. (2) as discussed by Revil et al. (1999b).

Modelling of SP produced by flow in the vadose zone is a three-step process, as suggested by Sill (1983). First, solve the hydraulic problem to determine the effective water content profile S_w and its fluid pressure P; second, compute the SP cross-coupling coefficient C using Eq. (2) and the physical properties of the fluid and the rock, and third, solve the electrical problem to determine V using Eq. (1). This approach is analogous to that of Adler et al. (1997) who modelled SP variations induced by atmospheric pressure variations.

2.1. Hydraulic model of rainfall infiltration and evaporation

We applied this strategy to model the electrokinetic effect of water infiltration in the vadose zone caused by rainfall events. The first step is to compute the water content profile. We have followed here a classical approach, assuming that the soil is a homogeneous isotropic porous medium and that water flow is vertical and laminar, so that Darcy's law can be applied. Under these conditions, the flow is governed by (Philip, 1998)

$$\frac{\partial \theta}{\partial t} = \frac{\partial}{\partial z}\left(D\frac{\partial \theta}{\partial z}\right) - \frac{\mathrm{d}K}{\mathrm{d}\theta}\frac{\partial \theta}{\partial z} \tag{3}$$

where z is vertical coordinate (positive downward), θ is the volumetric water content, D is the moisture diffusivity ($\mathrm{m^2\,s^{-1}}$) and K is the soil hydraulic conductivity ($\mathrm{m\,s^{-1}}$). The moisture diffusivity is

$$D = K\frac{\mathrm{d}\psi}{\mathrm{d}\theta} \tag{4}$$

where ψ is the tension, pressure or capillary head (m). The hydraulic conductivity K is assumed to follow the law of Brooks and Corey (1964)

$$K = K_s\left(\frac{\theta - \theta_r}{\theta_s - \theta_r}\right)^{3+(2/\lambda_b)} \tag{5}$$

where K_s is the saturated hydraulic conductivity ($\mathrm{m\,s^{-1}}$) and λ_b is an empirical constant. The capillary head ψ is assumed to follow the law of Van Genuchten (1980)

$$\psi = \psi_b\left[\left(\frac{\theta - \theta_s}{\theta_s - \theta_r}\right)^{-c/\lambda_v} - 1\right]^{1/c} \tag{6}$$

where ψ_b is the air entry head (m), C and λ_v are empirical coefficients, θ_r is the residual volumetric water content and θ_s is the volumetric water content in the saturated soil. Instead of using the volumetric moisture content θ, we preferred to work with the effective water content

$$S_w = \frac{\theta - \theta_r}{\theta_s - \theta_r} \tag{7}$$

The initial condition is a constant water content at all depths, i.e. $S_w = S_{wi}$, at $t = 0$. The surface boundary condition at $z = 0$ is (Smith et al., 1993)

$$r(t) = K(\theta) - D(\theta)\frac{\partial \theta}{\partial z} \tag{8}$$

where r is the surface flux ($\mathrm{m\,s^{-1}}$), and the lower boundary condition at $z = z_l$ is $S_w = S_{wi}$. With these boundary conditions we solved Eq. (3) using an implicit finite-difference scheme.

To illustrate the above theory, we modelled the SP response of a 12 h long, 3 mm/h rainfall starting at $t = 0$ and followed by evaporation at a rate of 1 mm/day. The initial conditions were $S_{wi} = 0.6$, $z_l = 2$ m, and the hydraulic properties of the soil were $\lambda = 0.4, c = 1.35$, $\theta_s = 0.4, \theta_r = 0$, $K_s = 1$ mm/h, $\psi_b = -1$ m; these values come from laboratory measurements on a sandy loam (Doussan et al., pers. comm.). The resulting effective water content profiles S_w are shown in Fig. 2 for several depths (every 10 cm): we can clearly observe the progressive infiltration of the rainfall water that increases S_w. From about Day 5, the evaporation process becomes significant and the shallow water content decreases.

2.2. Streaming potential cross-coupling coefficient C

Knowing the effective saturation, we can compute the SP coupling coefficient C using Eq. (2). For a silica-dominated porous material filled with water of 1:1 monovalent electrolyte (e.g. NaCl, KCl, or KNO_3) and in the pH range 6–8,

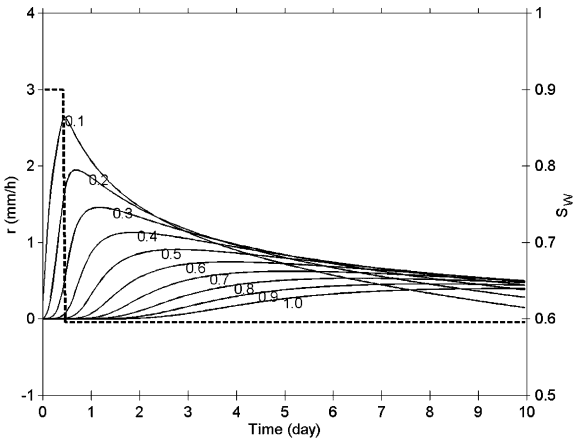

Fig. 2. Surface water flux r (dashed line in mm/h) and model of effective water content S_w (solid lines) for various depths (numbers on the figure, from 0.1 to 1 m every 0.1 m). We can clearly observe the progressive infiltration of the rainfall water that increases S_w. From about Day 5, the evaporation process becomes significant and the shallow water content decreases.

the ζ potential is (Revil and Pezard, 1999a)

$$\zeta = \frac{k_b T}{3e}\ln(C_f) + \frac{2k_b T}{3e} \ln\left(\frac{\sqrt{8.10^3 \varepsilon_f k_b T N}}{2e I_S^0 K} 10^{-pH}\right) \quad (9)$$

where C_f is the fluid salinity (mol l^{-1}), T is the temperature (K), k_b is Boltzmann's constant (1.381×10^{-23} J K^{-1}), e is the unit charge (1.6×10^{-19} C), N is Avogadro's number (6.02×10^{23} mol^{-1}), I_s^0 is the total surface site density (sites m^{-2}) and K is the dissociation constant of the reaction between silica grains and the electrolyte. The water electrical conductivity σ_f as a function of temperature and salinity is (Reppert, 2000)

$$\sigma_f = (5.6 + 0.27T - 1.5 \times 10^{-4} T^2) \times C_f - \frac{2 + 0.099T}{1 + 0.114 C_f} C_f^{3/2} \quad (10)$$

and the water dielectric permittivity ε_f is (Reppert, 2000)

$$\varepsilon_f = \varepsilon_c + A(1 - T/T_c)^{1-\alpha_c} \quad (11)$$

where A is constant, ε_f is the permittivity (F m^{-1}) at the temperature T_c (K), α_c is the critical exponent for isochoric heat capacity. We use $T_c = 25$°C and $\varepsilon_f = 78.5\ \varepsilon_0$ with $\varepsilon_0 = 8.85 \times 10^{-12}$ $C^2/(N\ m^2)$. The water dynamic viscosity η_f depends on temperature as (Reppert, 2000)

$$\eta_f = \eta_{20} \exp\left(-\ln 10 \frac{1.37023(T-20) + 8.36 \times 10^{-4}(T-20)^2}{109 + T}\right) \quad (12)$$

where T is the temperature (°C) and η_f is the dynamic viscosity at 20 °C (10^{-3} Pa s).

We combined Eqs. (2), (9), (10)–(12) to obtain the water content dependence of the SP coupling coefficient C (Fig. 3) of a sandy loam containing water of salinity of 10^{-3} mol l^{-1}, pH = 7, and a temperature of 15 °C. The C values for very low water contents are not shown because for these cases our assumption of a negligible surface electrical conductivity is no longer valid. We have plotted C in mV/m instead of V/Pa to ease the interpretation; the difference between this C and the C from Eq. (1) is only a factor ρg (10^4 Pa m^{-1}). C decreases with increasing water content, as observed by Morgan et al.

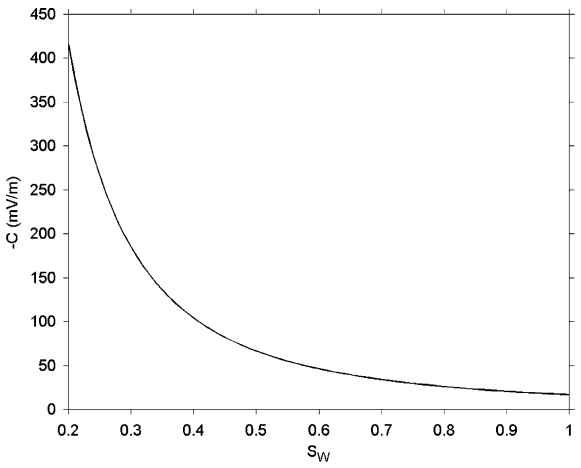

Fig. 3. Minus streaming potential coupling coefficient C (mV/m) as function of water content S_w for sandy loam (silica-dominated porous material) containing water of salinity of 10^{-3} mol l^{-1}, pH = 7, and temperature of 15 °C (formulae from Revil and Pezard, 1999a; Reppert, 2000). C decreases with increasing water content, this is because air does not greatly affect the water flow, but has a great influence on the electric conduction current by decreasing the electrical conductivity of the porous medium.

(1989) when they introduced air bubbles in water flowing through crushed granite. This is because air does not greatly affect the water flow (i.e. the convection current), but has a great influence on the conduction current by decreasing the electrical conductivity of the porous medium. As the electric charge conservation in the porous medium requires that the conduction current balances the convection current (Eq. (1)), the electric potential must increase to compensate the decrease of electrical conductivity and hence larger C is needed.

We computed C for our model of rainfall infiltration and evaporation (Fig. 4) using the modelled effective water content profiles and Eqs. (2), (9), (10)–(12); we assumed that the porous material was sandy loam (a silica-dominated material) filled with water of salinity of 10^{-3} mol l^{-1}, pH = 7, and temperature of 15 °C. As expected, C decreases during the infiltration phase when the water content increases, whereas C increases during the evaporation phase. The average value of C is around −40 mV/m; therefore unsaturated water flow, with hydraulic gradient up to several meters, generates SP variations of several millivolts that are easily recordable.

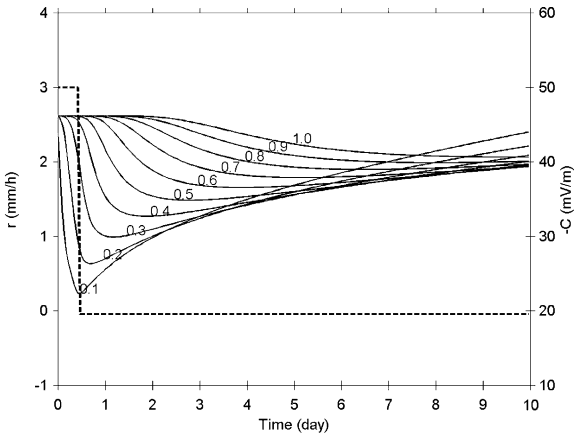

Fig. 4. Surface water flux r (dashed line in mm/h) and model of minus streaming potential coupling coefficient C (solid lines in mV/m) for various depths (numbers on the figure, from 0.1 to 1 m every 0.1 m). C decreases during the infiltration phase when the water content increases, whereas C increases during the evaporation phase. The average value of C is around −40 mV/m; therefore unsaturated water flow, with hydraulic gradient up to several meters, generates SP variations of several mV that are easily recordable.

2.3. Streaming potential model of rainfall infiltration and evaporation

As a third and final step, we solved Eq. (1) to compute the SP distribution in the vadose zone corresponding to the hydraulic and coupling coefficient models described above. As electrical signals are recorded between two electrodes, we calculated the SP distribution with respect to a reference electrode. The solution of Eq. (1) is then

$$\Delta V(z) = V(z) - V_{\text{ref}} = \int_{\text{ref}}^{Z} C(z') \frac{\partial \psi(z')}{\partial z} \mathrm{d}z' \qquad (13)$$

where z is the depth of the measurement electrode (m), V_{ref} is the electric potential at the reference electrode (V), and ψ is the capillary head (m). We assumed that the reference electrode was located at a depth of 2 m, i.e. under the maximum depth of infiltration. The resulting time evolution of SP is shown in Fig. 5 as a function of depth. We observe that the SP follows a downward diffusive process as expected from Eq. (3). SP values are negative because the electric currents are flowing upwards, i.e. in the opposite direction of the flow (Helmholtz–Smoluchowski Eq. (1)). The maximum SP anomaly is right at the end of the rainfall

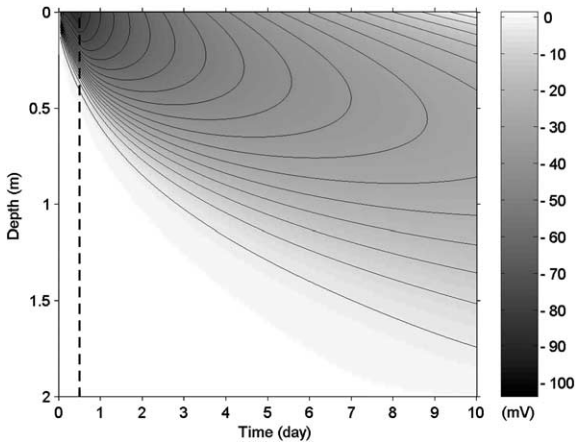

Fig. 5. Model of SP (mV) as function of time and depth during a 36 mm rainfall infiltration followed by evaporation; the reference electrode is at 2 m depth. The dashed vertical line indicates the end of the rainfall. SP values are negative because the electric currents are flowing upwards, i.e. in the opposite direction of the flow. The maximum SP anomaly is right at the end of the rainfall event (−100 mV after 12 h) in the first few centimeter of the soil, where water flow (and hence electrokinetic effects) is the strongest.

event (−100 mV after 12 h) in the first few centimeters of the soil, where water flow (and hence electrokinetic effects) is the strongest. After the end of the rainfall and during the evaporation phase, the maximum SP anomaly migrates downward and decreases in magnitude with time because of the combined effects of evaporation and ongoing infiltration at greater depths. Nevertheless, the SP is still around −30 mV at 50 cm depth 10 days after the end of the rainfall are, i.e. easily measurable. Therefore, our model shows that the infiltration and evaporation of rainwater generate detectable SP signals that exhibit the same dynamics as the water flow.

To compare with field conditions, we computed the time variations of SP recorded between two electrodes within the infiltration zone at depths of 40 and 30 cm, respectively (Fig. 6b). We also computed the water flux between these depths (Fig. 6a) from Darcy's law. Positive SP signals occur during the infiltration phase when the water flux is downwards. After the passage of the wetting front (7 h after the end of the rainfall), the SP and the flux decrease, then vanish together around Day 5; this corresponds to the change in hydraulic regime from water input to water extraction. Evaporation then dominates and both flux and SP become negative. Therefore, the sign of SP signals is a good indicator of the nature of the hydraulic transfers in the vadose zone.

Comparison of Fig. 6a and b reveals that the maximum SP occurs 4 h earlier than the maximum flux. This time delay is caused by stronger relative variations of the hydraulic conductivity K than of the electrokinetic coupling coefficient C during the water infiltration (Fig. 7b and c): indeed, K is multiplied by a factor of 5 whereas C decreases only by a factor 0.6. As both K and C multiply the capillary head gradient (in Darcy's law for K and Eq. (13) for C), SP follows more closely the capillary head gradient than, i.e. SP is in phase with the capillary head gradient while

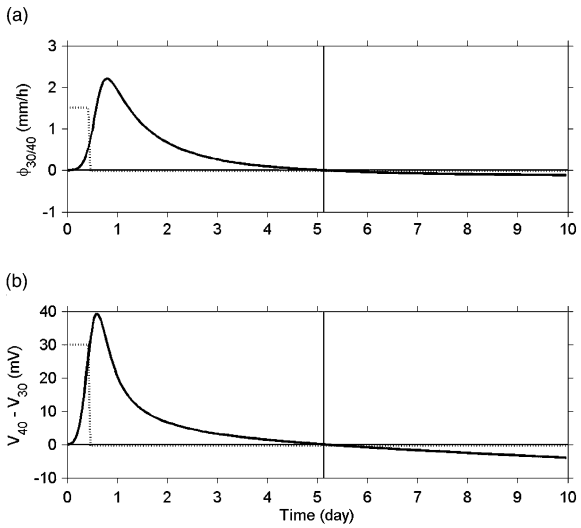

Fig. 6. (a) Unsaturated water flux $\Phi_{30/40}$ (mm/h) between 30 and 40 cm depth estimated using Darcy's law for a 36 mm rainfall infiltration followed by a constant evaporation of 1 mm/day, the dotted line is the surface water flux (mm/h) divided by 2 and the vertical line is when $\Phi_{30/40} = 0$; (b) electric potential difference ($V_{40} - V_{30}$ in mV) between the electrodes at 40 and 30 cm depth, the dotted line is the surface water flux (mm/h) multiplied by 10 and the vertical line is when $V_{40} = V_{30}$. Comparison of Fig. 6a and b reveals that the maximum electric potential difference occurs 4 h earlier than the maximum flux.

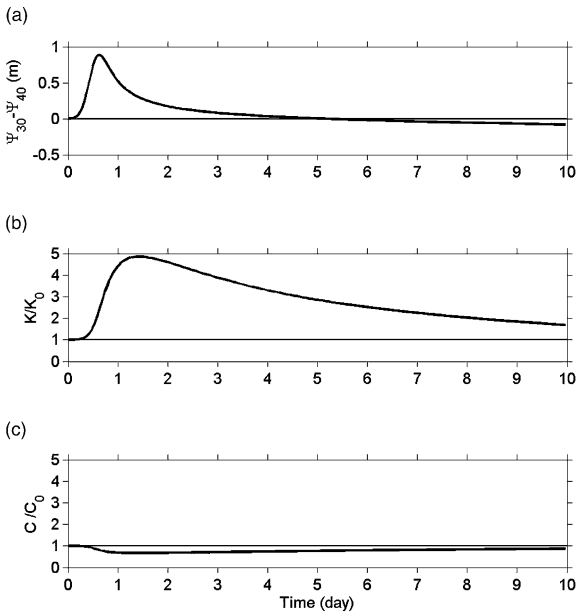

Fig. 7. (a) Capillary head (m) at 30 cm depth (ψ_{40}) minus at 40 cm depth (ψ_{30}); (b) ratio between the hydraulic conductivity K at 35 cm depth and K at day 0 at 35 cm depth; (c) ratio between the electrokinetic coupling coefficient C at 35 cm depth and C at day 0 at 35 cm depth. The hydraulic conductivity K has a stronger relative variation than the electrokinetic coupling coefficient C during the water infiltration: indeed, K is multiplied by a factor of 5 whereas C decreases only by a factor 0.6.

the unsaturated water flux is not (Fig. 7). Therefore, SP is a good indicator of the capillary head gradient but not of the unsaturated water flux.

To gain more insight into the long-term relationship between SP and water flux, we modelled the effects of a sequence of four successive 12 h rainfalls of 24 mm with 3-day long evaporation phases of 1 mm/day in between. The resulting water flux is shown in Fig. 8a and the SP signal in Fig. 8b: here also, the positive SP values coincide with infiltration phases (positive fluxes) and the negative SP values with phases of water loss (negative fluxes). This is indeed expected since wet soils are hydraulically conductive, resulting in a more effective evaporation,

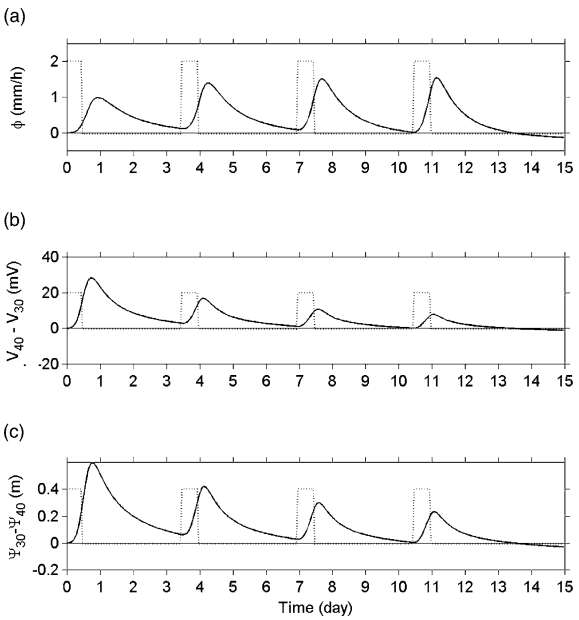

Fig. 8. (a) Unsaturated water flux Φ (mm/h) between 30 and 40 cm depth estimated using Darcy's law during a sequence of 24 mm rainfalls, the dotted line is the surface water flux (mm/day); (b) electric potential difference ($V_{40}-V_{30}$ in mV) between electrodes situated at 40 cm and 30 cm depth, the dotted line is the surface water flux multiplied by 10; (c) capillary head ($\psi_{30}-\psi_{40}$ in mV) at 30 cm depth minus the one at 40 cm depth, the dotted line is the surface water flux divided by 5. The maximum water flux after each rainfall increases throughout the rainfall sequence because the soil water content is increasing. On contrary, the maximum electric potential difference after each rainfall decreases throughout the rainfall sequence because the gradient of capillary head is decreasing.

hence the water flux is negative after the fourth rainfall event. The same reasoning applies to SP data.

The maximum water flux after each rainfall (Fig. 8a) increases throughout the rainfall sequence because the soil water content is increasing. On contrary, the maximum SP after each rainfall (Fig. 8b) decreases throughout the rainfall sequence because the gradient of capillary head is decreasing (Fig. 8a). Therefore, here again, SP is in phase with capillary head gradient while unsaturated water flux is not since the former does not depend directly on hydraulic conductivity variations. This lack of dependency is expected from the theory: in our model, the electrokinetic coupling in the soil follows the Helmholtz–Smoluchowski relation (Eq. (1)) in which there is no hydraulic conductivity term (K), so that C, and hence SP, are independent of K. A numerical study of SP in heterogeneous networks (Bernabé, 1998) showed that this is not always the case and that C at the flow scale may sometimes depend on K. It has also been observed experimentally that C in rocks (granite and sandstone) is approximately proportional to the square root of the permeability (Yoshida, 2001). In soils, K is related to the water salinity because the state of the EDL at the rock matrix interface changes (Fetter, 1992), and so do the ζ potential and C. Therefore, both theoretical and experimental works suggest that in heterogeneous media (like soils), electrokinetic processes are related to K. In this case, a thorough analysis of SP measurements may allow to characterize both hydraulic head and K variations that suffice to describe completely water fluxes in soils.

3. Case studies

We now compare the results of our model of SP variations induced by rainfall infiltration and evaporation to two SP data sets recorded after rainfall events in two different kinds of soil and climatic conditions: SP monitoring after a single rainfall on a glacial terrace (Thony et al., 1997) and SP monitoring in a lysimeter filled with sandy loam (Doussan et al., 2002). We have not attended to model the actual measurements because we do not have the soil parameters necessary for relevant modelling. We limit ourselves to first-order features in their data and in our 'generic' model.

3.1. Single rainfall in a glacial terrace

Thony et al. (1997) presented results from SP and hydraulic head monitoring over 10 days on a glacial terrace after a 23.8 mm rainfall event. From these measurements, they calculated the time evolution of zero-flux depth (Fig. 9a) that indicates the growth of the evaporation zone. The electric potentials were continuously recorded at depths 0.3, 0.5, 0.7 and 0.8 m. On Fig. 9b, we show the electric potential difference between the electrodes at 0.5 and 0.3 m: this will document the electrokinetic effect of the water flow at around 0.4 m depth. Moreover, to compensate for the electrode polarization, we fix the electrode potential difference at 0 mV before the rainfall.

As predicted from our model, the electric potential difference is positive during the infiltration phase. As soon as the regime changes to evaporation at the depth of the shallower electrode (Day 5 when the zero-flux is at 0.3 m depth), it becomes negative. This example illustrates that SP measurements are indeed describing the direction of the water flux occurring in the vadose zone at the depth of the electrodes.

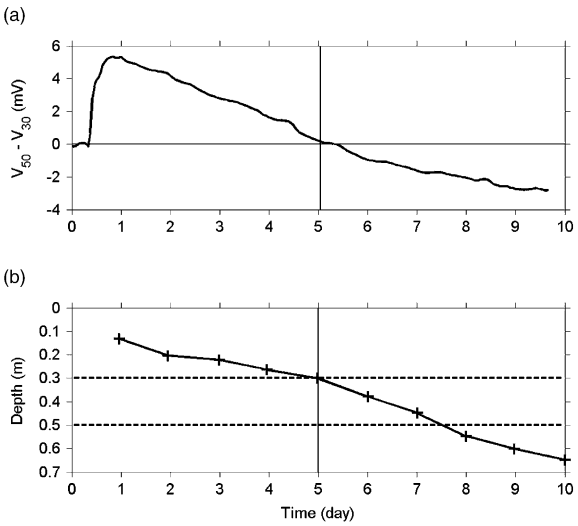

Fig. 9. (a) Electric potential difference ($V_{50} - V_{30}$ in mV) recorded by Thony et al. (1997) between electrodes at 50 and 30 cm depth after a 23.8 mm rainfall event occurring at day 0, the vertical solid line indicates when the potential difference is zero after the rainfall; (b) zero flux depth (crosses) calculated by Thony et al. (1997) after a 23.8 mm rainfall, the vertical solid line indicates when the zero depth is 0.3 m, the two dotted horizontal lines show the position of the electrodes. The electric potential difference is positive during the infiltration phase and as soon as the regime changes to evaporation at the depth of the shallower electrode (Day 5 when the zero-flux is at 0.3 m depth), it becomes negative.

3.2. Rainfall sequence in sandy loam

Doussan et al. (2002) recorded SP variations for 6 months to investigate the relationship between SP and unsaturated water flow over variable weather conditions. They monitored hydraulic heads with tensiometers and SP with unpolarizable electrodes at 30 and 40 cm depth within a lysimeter filled with sand. From these recordings and laboratory measurements of hydraulic conductivity, they calculated the soil water flux at 35 cm depth. From this unique data set, we focus here on a 50-day period during which several large rainfall events occurred. The time series of the electric potential difference (Fig. 10a) and the water

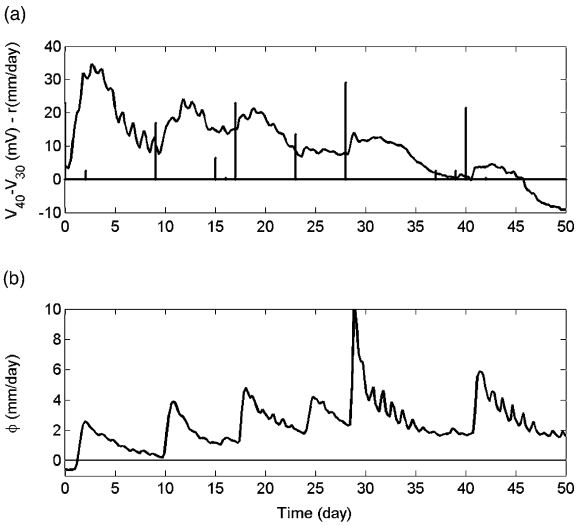

Fig. 10. (a) Electric potential signal (solid line, $V_{40} - V_{30}$ in mV) recorded by Doussan et al. (2002) during a sequence of rainfall events r (bars in mm/day) between electrodes at 40 and 30 cm depth; (b) soil water fluxes Φ (m) at 35 cm depth calculated by Doussan et al. (2002) from the hydraulic conductivity and hydraulic heads data. The electric potential difference and the water flux show a strong correlation to rainfall events. The electric potential difference increases quickly then decreases gradually after each rainfall event, just like the water flux, but the latter is delayed by several hours. In addition, after several rainfall events, evaporation becomes more efficient and SP vanishes or even becomes negative at the depth of the upper electrode (after Day 40).

flux (Fig. 10b) show a strong correlation to rainfall events. The electric potential difference increases quickly then decreases gradually after each rainfall event, just like the water flux, but the latter is delayed by several hours as expected from our model. In addition, after several rainfall events, evaporation becomes more efficient and SP vanishes or even becomes negative at the depth of the upper electrode (after Day 40) just like in our model (Fig. 8). However, here, water flux remains always positive in contradiction with our model.

This difference may be in part related to the effects of small-scale heterogeneities on local capillary head measurements. To illustrate these effects, hydraulic heads measured at two different locations within the lysimeter but at the similar depths are shown in Fig. 11. There are significant differences that could be caused by preferential flow paths within the vadose zone due to macropores, fingering or funnelling (Fetter, 1992). In addition, cumulative effects of rainfall and potential evapotranspiration (Doussan, pers. comm., Fig. 12) indicate that after day 35, there is a strong deficit of water that should produce a strong

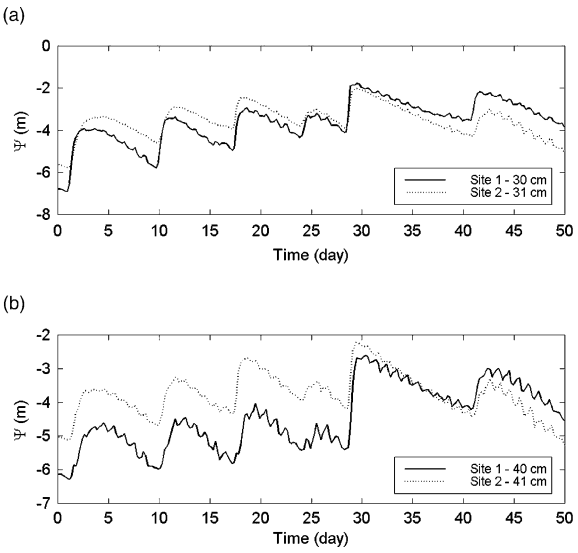

Fig. 11. (a) Capillary head ψ (m) recorded at 30 cm (solid line) and 31 cm (dotted line) depth recorded by Doussan et al. (2002) at two places of the lysimeter; (b) capillary head ψ (m) recorded at 40 cm (solid line) and 41 cm (dotted line) depth recorded by Doussan et al. (2002) at two places of the lysimeter. The differences illustrate the degree of hydraulic heterogeneity within the lysimeter.

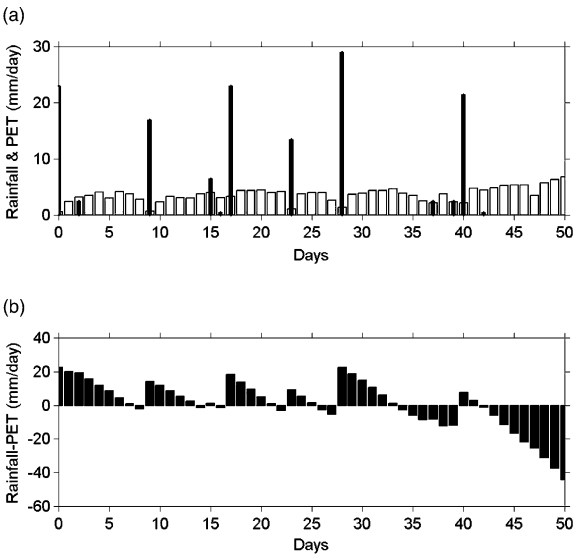

Fig. 12. (a) Rainfall (black bars in mm/bar) and potential evapotranspiration (white bar, PET in mm/day); (b) cumulative rainfall minus cumulative potential evapotranspiration (PET) per day (mm/day). Unpublished data, courtesy of C. Doussan. Note that evapotranspiration dominates from Day 35.

evaporation phase, i.e. negative water fluxes at the depth of the upper electrode. Therefore, as the calculated water flux is always positive (Fig. 10b), we suggest that the local determination of flux may not be representative of the overall unsaturated soil water flux.

The difference in the actual nature of tensiometric and SP measurements has to be taken into account when considering their joint interpretation. Indeed, tensiometric measurements require a good *hydraulic* coupling between the sensor and the *flow* that is sometimes difficult to obtain because of soil heterogeneity. On the opposite, SP requires a good *electrical* coupling between the electrode and the *soil*; this is usually the case because because we usually add a saline clay solution around the electrode to ensure good electrical coupling. Therefore, if one installs several electrodes close to flow but in a zone with a bad hydraulic connection to it, they may record more meaningful signals than tensiometers.

This could be the case for the data shown on Fig. 10. There, it seems likely that the hydraulic head measurements only describe the dynamics of flow in the vicinity of the tensiometer whereas the SP

measurements are describing the direction of the water flux at the scale of the electrode separation (10 cm). This may explain why the SP measurements are not exactly compatible with the observed local unsaturated soil water flux.

4. Conclusion

Field estimation of soil water flux has a direct application for water resource management. Standard methods are often difficult to apply because of the heterogeneity of the subsurface. In the present study, we have shown that SP monitoring can provide a cost-effective tool to help estimate the nature of the hydraulic transfers (infiltration or evaporation) in the vadose zone. In addition, SP measurements allow to characterize the upward or downward direction of water flux at the scale of the electrode separation (usually several decimetres), i.e. at a much larger scale than tensiometric measurements. Moreover, as SP coupling coefficients are related to the nature and concentration of solutes, SP could be used in the future to characterise contaminant fluxes in soils. However, a detailed description of the electrokinetic phenomena taking into account soil heterogeneity is necessary to better characterize electrokinetic effects at the decimetric scale.

Acknowledgements

This study benefited from a grant INSU-CNRS 'Programme National de Recherche en Hydrologie (PNRH)'. We want to thank Claude Doussan and Laurence Jouniaux for providing us their data. We also want to thank the two referees and the editor for their fruitful comments, Philippe Ackerer and Pascal Sailhac for fruitful discussions. MD wishes to acknowledge financial support from joint CNRS-Région Alsace doctoral fellowship. This is EOST publication No. 2003. 038-UMR7516.

References

Adler, P.M., Thovert, J.F., Jacquin, C., Morat, P., Le Mouël, J.L., 1997. Electric signals induced by the atmospheric pressure variations in unsaturated media. C. R. Acad. Sci. Paris 324, 711–718.

Bernabé, Y., 1998. Streaming potential in heterogeneous networks. J. Geophys. Res. 103, 20827–20841.

Brooks, R.H., Corey, A.T., 1964. Hydraulic properties of porous media. Hydrol. Pap. 3, Colo. State Univ., Fort Collins.

Bogoslovsky, V.A., Ogilvy, A.A., 1970. Natural potential signals as a quantitative index of the rate of seepage from water reservoir. Geophys. Prospect. 18, 261–268.

Bogoslovsky, V.A., Ogilvy, A.A., 1973. Deformations of natural electric fields near drainage structures. Geophys. Prospect. 21, 716–723.

Doussan, C., Jouniaux, L., Thony, J.L., 2002. Variations of self potential and unsaturated water flow with time in sandy loam and clay loam soils. J. Hydrol. 267, 173–185.

Fetter, C.W., 1992. Contaminant Hydrogeology, Macmillan, New York, USA.

French, H.K., Hardbattle, C., Binley, A., Winship, P., Jakobsen, L., 2002. Monitoring snowmelt induced unsaturated flow and transport using electrical resistivity tomography. J. Hydrol. 267, 273–284.

Hagrey, S.A., Michaelsen, J., 1999. Resistivity and percolation study of preferential flow in vadose zone at Bokhorst, Germany. Geophysics 64, 746–753.

Hagrey, S.A., Schubert-Klempnauer, T., Wachsmuth, D., Michaelsen, J., Meissner, R., 1999. Preferential flow: first results of a full-scale flow model. Geophys. J. Int. 138, 643–654.

Herrmann, K.H., Pohlmeier, A., Gembris, D., Vereecken, H., 2002. Three-dimensional imaging of pore water diffusion and motion in porous media by nuclear resonance imaging. J. Hydrol. 267, 244–257.

Kemna, A., Vanderborght, J., Kulessa, B., Vereecken, H., 2002. Imaging and characterisation of subsurface solute transport using electrical resistivity tomography (ERT) and equivalent transport models. J. Hydrol. 267, 125–146.

Legchenko, A., Baltassat, J.M., Beauce, A., Bernard, J., 2002. Nuclear magnetic resonance as a geophysical tool for hydrogeologists. J. Hydrol. 267, 21–46.

Morgan, F.D., Williams, E.R., Madden, T.R., 1989. Streaming potential properties of Westerley granite with applications. J. Geophys. Res. 94, 12449–12461.

Ogilvy, A.A., Ayed, M.A., Bogoslovsky, V.A., 1969. Geophysical studies of water leakages from reservoirs. Geophys. Prospect. 17, 36–62.

Petiau, G., 2000. Second generation of lead–lead chloride electrodes for geophysical applications. Pure Appl. Geophys. 157, 357–382.

Philip, J.R., 1998. Infiltration into crushed soils. Water Resour. Res. 34 (8), 1919–1927.

Reppert, P.M., 2000. Electrokinetics in the Earth. Ph.D. thesis. Mass. Inst. Tech.

Revil, A., Pezard, P.A., 1999a. Streaming potential in porous media 1. Theory of the zeta potential. J. Geophys. Res. 104, 20033–20048.

Revil, A., Schwaeger, H., Cathles, L.M. III, Manhardt, P.D., 1999b. Streaming potential in porous media, 2. Theory and application to geothermal systems. J. Geophys. Res. 104, 20033–20048.

Schmalz, B., Lennartz, B., Wachsmuth, D., 2002. Analyses of soil water content variations and GPR attribute distributions. J. Hydrol. 267, 217–226.

Sill, W.R., 1983. Self-potential modeling from primary flows. Geophysics 48, 76–86.

Smith, R.E., Corradini, C., Melone, F., 1993. Modeling infiltration for multistorm runoff events. Water Resour. Res. 29 (1), 133–144.

Stoffregen, H., Yaramanci, U., Zenker, T., Wessolek, G., 2002. Accuracy of soil water content measurements using ground penetrating radar: comparison of ground penetrating radar and lysimeter data. J. Hydrol. 267, 201–206.

Thony, J.L., Morat, P., Vachaud, G., Le Mouël, J.L., 1997. Field characterization of the relationship between electrical potential gradients and soil water flux. C. R. Acad. Sci. Paris 325, 317–321.

Titov, K., Ilyin, Yu., Konosavski, P., Levitski, A., 2002. Electrokinetic spontaneous polarization in porous media: petrophysics and numerical modelling. J. Hydrol. 267, 207–216.

Van Genuchten, M.T., 1980. A closed-form equation for predicting the hydraulic conductivity of unsaturated soils. Soil Sci. Soc. Am. J. 44, 892–898.

Yoshida, S., 2001. Convection current generated prior to rupture in saturated rocks. J. Geophys. Res. 106, 2103–2120.